

Photoproduction of Positive Pions from Hydrogen near Threshold

G. M. LEWIS, R. E. AZUMA,* E. GABATHULER,† D. W. G. S. LEITH, AND W. R. HOGG‡

Department of Natural Philosophy, The University, Glasgow, Scotland

(Received August 31, 1961)

The variation of the differential cross section for π^+ photoproduction from hydrogen, with γ -ray energy, has been examined at a laboratory angle of 58° to the γ -ray beam. A thin hydrogen target, and a counter system designed to eliminate random events, have been employed. Mean values for the differential cross section $d\sigma/d\Omega$ at γ -ray energies of 162, 168, 175, and 192 Mev are 5.42 ± 0.38 , 5.77 ± 0.41 , 6.74 ± 0.47 , and $8.22 \pm 0.58 \mu\text{b/sr}$, respectively, where the error limits refer to relative values. The results substantiate the rising trend of the interaction quantity $\{(\mu^2/p\epsilon)(1+\omega/M)^2\}$ near threshold, in accord with dispersion theory; and the absolute cross sections are compatible with a threshold value for a_0^+ near $20 \mu\text{b/steradian}$, consistent with findings in related pion work.

1. INTRODUCTION

THE threshold region of π^+ -meson photoproduction is one of intrinsic significance and bears importantly on an understanding of pion physics. Its study can lead to a determination of the pion-nucleon coupling constant, and the process can be linked up with other low-energy pion phenomena.

One of the main observed characteristics in this region is the approximately linearly momentum-dependent pion emission and isotropic distribution (cf. Beneventano *et al.*¹). This is associated with the dominant role, in the process, of the zero angular momentum state. This is in essential accord with both pseudo-scalar classical and field theory. More precisely in center-of-mass coordinates, the differential cross section $d\sigma/d\Omega$ would be expected to obey a relation of type

$$\frac{1}{p\epsilon} \left(1 + \frac{\omega}{M}\right)^2 \frac{d\sigma}{d\Omega} = \frac{2e^2 f^2}{\mu^2} \left[\frac{1}{\omega\epsilon} \left(1 - \frac{\mu^2}{2\omega^2} \frac{p^2 \sin^2\theta}{(\epsilon - p \cos\theta)^2} - \frac{\epsilon - p \cos\theta}{M + \omega}\right) \right] \quad (1)$$

(cf. Foldy² and Moravcsik³). The right-hand side of this expression is proportional to the square of the matrix element, H , of the transition. In this form the nucleon mass has been approximated by the nucleon rest mass M . Here p is the momentum, and ϵ the total energy of the pion of rest mass μ , ω is the γ -ray energy, θ is the angle of pion emission, all in center-of-mass coordinates; c is taken as unity. The expression $(\mu^2/p\epsilon)(1+\omega/M)^2 d\sigma/d\Omega$, could therefore be expected to show a slight rise with energy near threshold for θ close to 90° .

Subsequently the rise of this quantity with energy near threshold has been predicted by the single dis-

persion theory (Chew *et al.*⁴), and a somewhat similar rise is also predicted by the Mandelstam dispersion representation (cf. Fig. 8). It is desirable to check precisely on these predicted trends. Moreover the possible existence of an underlying π - π interaction should be explored (cf. Ball⁵), and its strength delimited. This can be achieved through the study of π^+ photoproduction and the π^-/π^+ ratio.

The behavior near threshold can be associated with other aspects. A knowledge of the π^+ photoproduction cross section together with data on the π^-/π^+ photoproduction ratio from deuterium near threshold (after including interaction corrections), can lead by detailed balancing to the cross section of the inverse reaction $\pi^- + p \rightarrow \gamma + n$. From the Panofsky ratio an estimate can then be made of the charge exchange scattering $\pi^- + p \rightarrow \pi^0 + n$, and of the S -wave scattering phase shifts. Comparison with experimental values for the latter serves to check the over-all consistency of the field. Reference should also be made to the work of Gatti *et al.*,⁶ which gives direct information on the process $\pi^- + p \rightarrow \gamma + n$.

Experimentally it is difficult to make measurements in the threshold region because the differential cross section is falling off, the pions have little penetrating power; and at forward angles, where the measurements are made to take advantage of the kinematics, the electron and γ -ray backgrounds are intense. In an earlier publication (Lewis and Azuma⁷), a new counter method was described for detecting, unambiguously, photoproduced π^+ mesons near threshold. The potentialities of the method were investigated and values for cross sections were obtained by a CH_2 -C subtraction technique, but further studies were necessary to determine more exactly the trend with energy. This counter method has been developed further, and a thin hydrogen target of special design has been constructed, so that a more precise study could be made of the low-

* Now at Physics Department, University of Toronto, Canada.

† Now at Laboratory of Nuclear Studies, Cornell University, Ithaca, U. S. A.

‡ Now at CERN, Geneva, Switzerland.

¹ M. Beneventano, G. Bernardini, D. Carlson-Lee, G. Stoppini, and L. Tau, *Nuovo cimento*, **4**, 323 (1956).

² L. L. Foldy, *Phys. Rev.* **76**, 372 (1949).

³ M. J. Moravcsik, Brookhaven National Laboratory Report 459-T-100, 1957 (unpublished).

⁴ C. F. Chew, M. L. Goldberger, P. E. Low, and Y. Nambu, *Phys. Rev.* **106**, 1345 (1957).

⁵ J. S. Ball, University of California Radiation Laboratory Report UCRL-9172, TID 4500, 1960 (unpublished).

⁶ G. Gatti, P. Hillman, W. C. Middelkoop, T. Yamagata, B. Zavattini, *Phys. Rev. Letters* **6**, 706 (1961).

⁷ G. M. Lewis and R. E. Azuma, *Proc. Phys. Soc. (London)* **73**, 873 (1959).

energy behavior at forward angles. A summary of the position in threshold photoproduction work up to 1959 was given by Bernardini at the Kiev Conference.⁸ In the meanwhile further work has been reported at the Rochester Conference (Rutherglen *et al.*⁹).

2. EXPERIMENTAL PROCEDURE

(a) General Arrangement

The over-all arrangement for the experiment is shown in Fig. 1. The bremsstrahlung beam was passed through an evacuated chamber and allowed to strike the liquid hydrogen target at an angle of 30° to the normal of the target. The photoproduced pions were observed at an angle of 58° to the initial bremsstrahlung beam direction. The details of the target are given in the next paragraph and Fig. 2.

The maximum energy to which the electrons were accelerated before being allowed to strike the internal tungsten target in the synchrotron, was 250 Mev throughout the experiment. By suitable modulation of the synchrotron rf power, the bremsstrahlung pulse could be lengthened to approximately 2 msec with only slight variation of the end-point energy. The bremsstrahlung beam was passed through a lead collimator and scrubber magnets before striking the target. The maximum diameter of the beam at the target was $1\frac{1}{4}$ in. The total energy content of the bremsstrahlung beam was measured with a Wilson-type quantameter.¹⁰

(b) Liquid Hydrogen Target

The target was designed so that a thin slice of liquid hydrogen with flat parallel sides was presented to the beam. The thickness of this slice was 1.47 cm measured optically to an accuracy of 0.3%. Compression rings, as shown in Fig. 2, were provided to keep the Melinex walls taut. In order to ensure that the walls of the

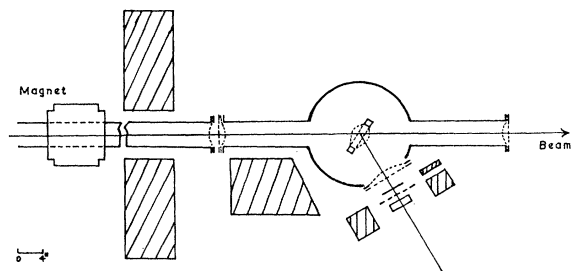


FIG. 1. General arrangement showing the γ -ray beam from the synchrotron, the thin hydrogen target, and the counter system.

⁸ G. Bernardini, *Ninth Annual Conference on High Energy Physics, Kiev 1959*. (Academy of Science, U.S.S.R., 1961).

⁹ J. G. Rutherglen, J. Walker, D. Miller, J. Patterson, *Proceedings of the 1960 Annual International Conference on High Energy Physics at Rochester* (Interscience Publishers, Inc., New York, 1960).

¹⁰ R. R. Wilson, *Nuclear Instr.* 1, 101 (1957).

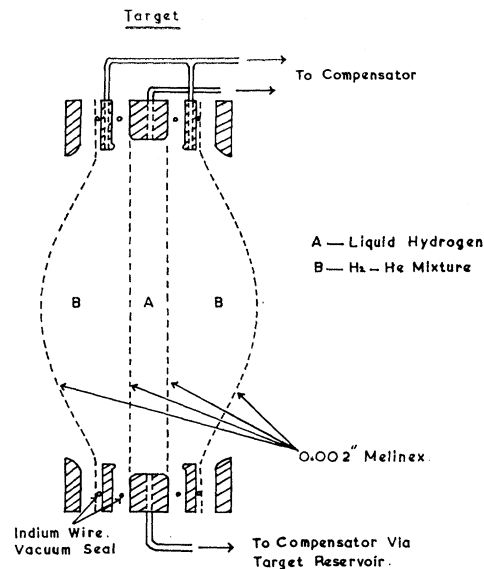


FIG. 2. Target chamber. This together with the compensator form a closed system independent of the main liquid hydrogen cryostat.

target remained flat under all experimental conditions, a special technique of compensation was developed.

The target itself consisted of a copper annulus, on both sides of which thin Melinex sheets were cemented with Araldite to form the target walls. A Melinex sheet was clamped to the outer surface of each compression ring and the enclosed space *B*, Fig. 2, was filled with a mixture of helium (4 cm Hg) and hydrogen (72 cm Hg) gases. The liquid hydrogen part of the target assembly is indicated by *A* in the diagram. The pressure of the gas mixture in *B* was always maintained exactly equal to the vapor pressure of the liquid hydrogen in *A* by the compensator, thus ensuring that the liquid hydrogen walls always remained accurately flat. The liquid was introduced into this target by liquefaction from dry hydrogen gas, and the whole assembly was maintained in thermal contact with a liquid hydrogen cryostat (cf. Bellamy, Hogg, and Miller¹¹).

The compensator consists of a thin rubber bladder contained within a glass sphere at room temperature. The sphere is connected to the vapor of the liquid hydrogen in *A*, and the bladder to the hydrogen-helium gas mixture in *B*. Any difference in pressure between *A* and *B* is immediately counteracted by inflation or deflation of the bladder.

A 0.003-in. thick Melinex sheet, through which the pions emerged, covered a port which was of large diameter (5.5 in.) to avoid small-angle pion scattering into the counter system. The γ -ray beam ports were covered with 0.001-in. Melinex. A similar sheet was attached to each port of the vacuum jacket forming a double wall. Dry nitrogen gas was passed through the

¹¹ E. H. Bellamy, W. R. Hogg, and D. Miller, *Nuclear Instr. Methods* 7, 293 (1960).

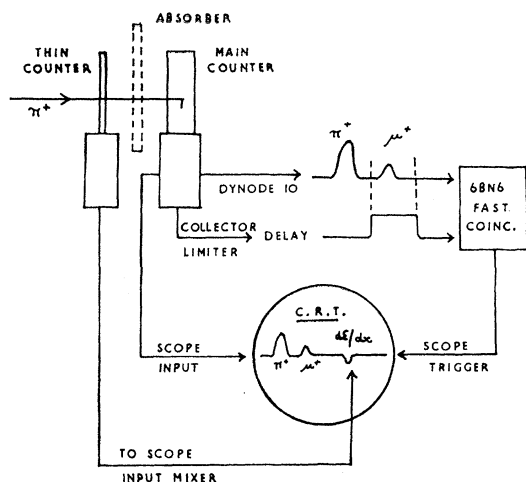


FIG. 3. Counter system: A π^+ particle passes through the thin front scintillator and enters the main counter where it decays giving a μ^+ pulse of fixed height. A coincidence between the μ^+ pulse (from dynode 10) and a delayed rectangular limiter pulse generated by the π^+ pulse (from the collector) triggers off a fast oscilloscope. The time related $\pi^+ \rightarrow \mu^+$ pulses from the 8th dynode of the main counter are then displayed on the trace, together with the one inverted dE/dx pulse produced by the passage of the π^+ through the front crystal.

space formed by the double wall to prevent condensation of water vapor on the 0.0006-in. aluminium walls of the radiation shield at liquid nitrogen temperature. In operation the consumption of liquid hydrogen from the cryostat was less than 1 liter per day

(c) Detection System

The π^+ mesons were detected and identified by a two-counter telescope system (cf. Fig. 3) which depends primarily on the decay characteristics of the π^+ meson, i.e., π^+ decaying into a μ^+ of unique energy, 4.15 Mev, with a lifetime of 2.55×10^{-8} sec. The method has been discussed in a previous paper.⁷ In the present experiment, however, an additional means of identification is provided by an examination of the rate of energy loss (dE/dx) of the π^+ meson in the front scintillator (a thin plastic sheet 0.025 in. thick). The second, or main counter has a 1-in. thick plastic scintillator in which the pions must stop in order to be detected. The optional insertion of a $\frac{1}{4}$ -in. copper absorber between the counters allows a higher energy group of pions to be detected. If then, a pion stops in the main counter after having first passed through the thin counter, and if the decay μ^+ is also stopped in the main counter and appears within a time gate about 1.7 to 5.0×10^{-8} sec after the appearance of the pion, the electronics is such as to cause a cathode-ray tube display (Tektronix 517A) of the π^+ and μ^+ main counter pulses to be photographed. The thin-counter π^+ pulse appears inverted and delayed by a fixed amount relative to the main-counter π^+ pulse (cf. Fig. 3.). The main-counter display pulses are obtained from the 8th dynode of the

photomultiplier. Pulses from the 10th dynode lead to a distributed amplifier and then to one channel of the 6BN6 coincidence box. Pulses from the collector are shaped by a limiter valve and thence through delay cable to the other channel of the coincidence box.

One of the main difficulties in obtaining a precise value for the differential cross section in this type of experiment has been the difficulty in positively excluding, or accurately subtracting, those events which can simulate true $\pi^+ \rightarrow \mu^+$ events (cf. the discussion by Lewis and Azuma⁷). A typical $\pi^+ \rightarrow \mu^+$ display is sketched in Fig. 3. Displays similar to this can appear which are due to random coincidences (cf. Fig. 5.). A random event of this type can only be due to a charged particle followed by a γ ray producing a pulse height comparable to that of a 4.15-Mev decay μ^+ . Since these are random events, the "inverse" of these should occur in equal numbers i.e., a γ ray giving the μ^+ pulse height followed by a charged particle. This has provided, in the past, the basis for the random subtraction. However, in the present setup, due to the inclusion of the dE/dx versus E criterion, the only significant type of random event which cannot be recognized immediately as such, in a run with no absorber between the counters, is one in which a meson (either a μ , or π^+ which does not decay within the required interval) is in the proper time coincidence with a γ ray. These events have been found to be very rare.

In this experiment the 0.025-in. NE 102 scintillator had a width of 2.06 in. and a height of 3.25 in. It was appropriately coupled by a thin perspex guide, to avoid Čerenkov effects, to a magnetically shielded RCA 7265 type photomultiplier. The 1-in. NE 102 main crystal, 2 in. wide \times 3 in. high was coupled to a magnetically shielded RCA 6342 photomultiplier. The photomultiplier output at the 8th dynode in the pulse-height region of interest had been previously shown to be linear as a function of light input with a 10^{-8} -sec light flashing apparatus. The thin and main scintillators were separated by $1\frac{1}{2}$ in., and the $\frac{1}{4}$ -in. thick copper absorber screen could be inserted in a fixed position between the two counters, when desired. The main counter was placed 13 in. from the target. Shielding blocks of lead and iron were set back so as to avoid possible pion scattering from them into the counter. With the absorber out differential cross sections were simultaneously determined for laboratory energies of 162, 168, and 175 Mev. With the absorber inserted the differential cross section was found for a laboratory γ -ray energy of 192 Mev. Runs with absorber in were regularly interspersed with runs with absorber out, throughout the experiment.

3. EXPERIMENTAL RESULTS

Figure 4 shows some photographs of film from an actual run with no absorber. It shows the two consecutive events of $\pi^+ \rightarrow \mu^+$ type which had been se-

FIG. 4. Some of the filmed $\pi^+ \rightarrow \mu^+$ traces observed with no absorber. (The pulses have a full width of about 10^{-8} sec at half height.)



lected by the time gate, with the second pulse of the appropriate μ^+ height.

The energy resolution capabilities of the thin front crystal had been initially proved to have a 30% half-width with the ~ 2 -Mev straight-through electrons from an In^{114} source, selected by a coincidence method. Figure 5 shows plots of the raw data from film obtained in a run without absorber. It shows how electron- γ ray events and their random inverses are located in the left-hand corner, and illustrates the unambiguous π^+ meson band, even at the lowest energies. On the basis of data of this type, events in the left-hand corner below the dashed line were discarded, as being due to electron γ -ray coincidences.

Figure 6 shows a time plot on a logarithmic scale of all π^+ mesons observed with an energy greater than 6 Mev. The edges of the gate are seen to be sharp. The number observed per unit time interval falls off with the 2.55×10^{-8} -sec lifetime (cf. Ashkin *et al.*¹²). The linearity of the time base was studied using a signal generator calibrated against the 95-Mc/sec. B.B.C. transmission. Separate time plots were also drawn up for various meson energy bands, and allowed an assessment of the time gate to be made, for all those meson energies considered for the final calculation. The time gate had been initially set up with a ThC'' source. These γ rays gave pulses on the Compton edge just smaller than the pulse height of the lowest energy pions of interest, and also just smaller than the μ^+ pulse height which operated the other channel of the coincidence unit. The efficiency of the gate and associated oscilloscope trigger setting was quantitatively checked in the following way using a thorium source. The delay cables to the coincidence unit were adjusted so that a single γ ray in the main counter triggered the oscilloscope in the usual manner. The thorium γ -ray spectrum from the display side was first exhibited on a 100-channel CDC kicksorter. Afterwards a second

spectrum was obtained when the kicksorter was gated by pulses derived from the time base of the oscilloscope for the working trigger setting. The full and partial spectra overlapped fully above certain energies. This process was carried out for varying delay cable lengths (cf. Fig. 3). The efficiency of the gate was shown to be 100% in the main operating region for the energies concerned. A monitoring check of this type was done at intervals throughout the time of the actual run. Further confirmation of 100% working efficiency was obtained by slightly lowering further the trigger setting and comparing pion production rates.

Figures 7(a) and (b) show the energy plots of π^+ mesons obtained directly from the analyzed films, with absorber out and in, respectively, for the run with liquid hydrogen. The emitted pion distribution can be obtained from the absorber out curve, when allowance is made for the kinematical factors and corrections referred to below. The "absorber in" curve refers to a fairly narrow, uniform band of high-energy pions; the

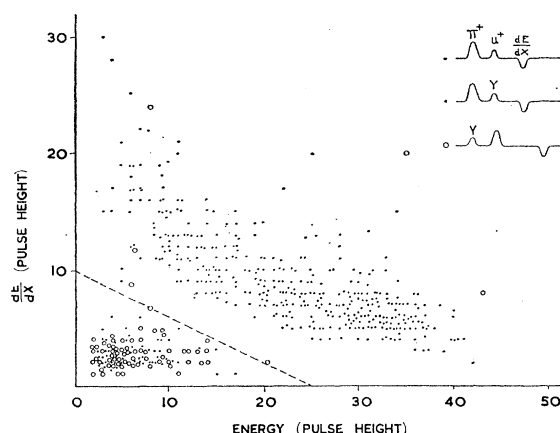


FIG. 5. A plot with no absorber of dE/dx (thin-counter pulse height) against E (main-counter pulse height) for all events (●) of $\pi^+ \rightarrow \mu^+$ type, showing the meson band. Random e, γ coincidences, and their inverses γ, e (○) are apparent in roughly equal numbers in the left-hand corner, and would cancel one another out, even without dE/dx selection.

¹² J. Ashkin, T. Fazzini, G. Fidecaro, Y. Goldschmidt-Clermont, W. H. Lipman, A. W. Merrison, and H. Paul, *Nuovo cimento* 16, 490 (1960).

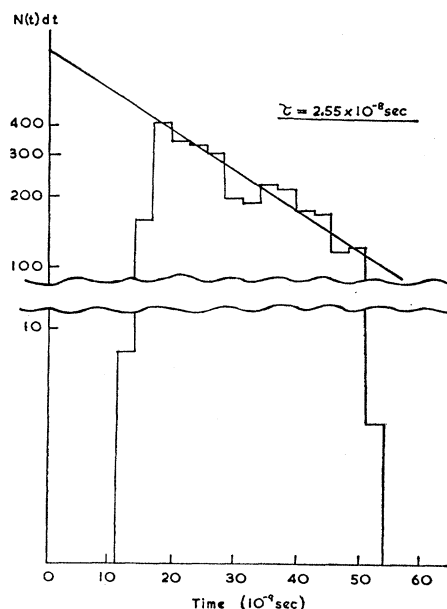


FIG. 6. A logarithmic distribution plot (for π^+ mesons of observed energy greater than 6 Mev) of the time separation between π^+ and μ^+ pulses, showing that the time gate accepted only those π^+ mesons which decayed between $\sim 1.7 \times 10^{-8}$ sec and 5×10^{-8} sec. The solid curve is a plot of the accepted lifetime (2.55×10^{-8} sec).

energy distribution, after energy losses in the copper, will be distorted in the general manner shown.

The apparatus was self-calibrating with respect to energy, and the 24-Mev energy point is that where the thickness of the 1-in. scintillator is equal to the range of the π^+ mesons and where half the μ^+ mesons register and half escape. The μ^+ pulse height is also shown. Each film could therefore be examined to confirm that there was no gain change. Rough subsidiary checks could also be obtained by photographing thorium pulses on the films. The μ^+ pulse height can be correlated with that of a π^+ of energy $(4.15 \times \pi^+ \text{ mass} / \mu^+ \text{ mass})$ by the Seitz relation (cf. Taylor *et al.*¹³). A small correction for nonlinearity of the scintillation response S was applied. We have taken $S \equiv E$ above; however dS/dx can be more properly assumed proportional to $(dE/dx)^{-1}$, which is consistent with known scintillation data.

The inverses in the meson band only occurred in the absorber out run and were very small in number (1% in all and fairly uniformly distributed in energy). It was deduced that dead-time losses were also very small. Long background runs were also taken, with the target emptied of liquid hydrogen, but with the cryostat still at liquid hydrogen temperature. These background runs were done before and after the main run, in each case with and without absorber. The background counting rate was of order 12% of the total counting rate.

¹³ C. J. Taylor, W. K. Jentschke, M. E. Romley, P. S. Ely, and P. G. Kruger, Phys. Rev. 84, 1031 (1951).

It was necessary to correct the energy plots obtained from the raw data. Corrections were made for solid-angle variations due to range difference, for π^+ decay in flight before the counters were reached, and minor corrections ($\sim 1\%$) due to μ^+ escape at the edges and $\mu^+ - e^+$ decay. Scattering out from the copper absorber was largely compensated by scattering in, for the pion energy band considered; and the same was true for the thin crystal. A small correction was applied for scattering in the main crystal; also for nuclear absorption (2%) in the copper absorber, when used.¹⁴

Detailed target corrections were carried out due to energy distortion of the pion energy spectrum by the

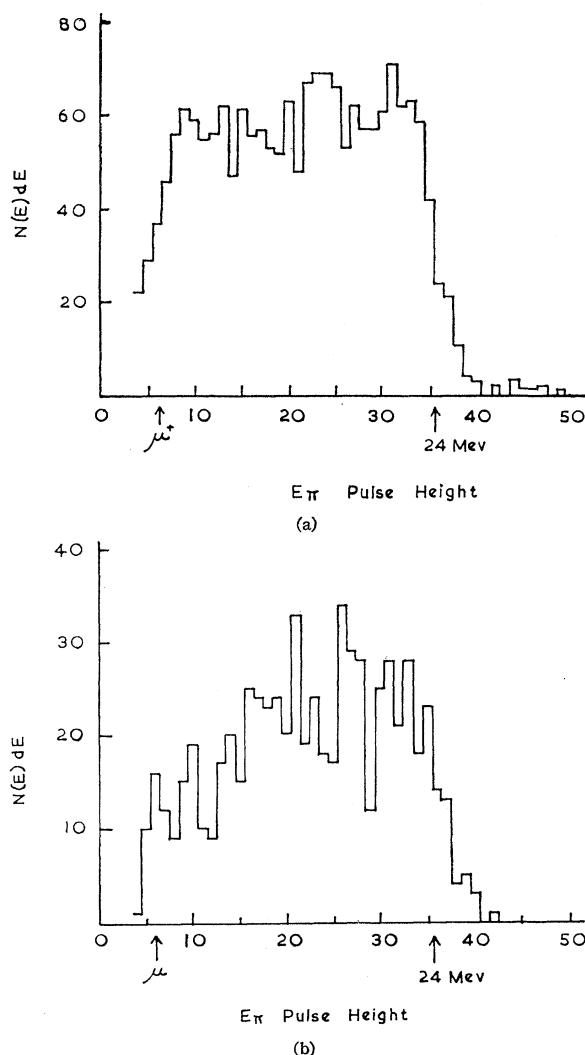


FIG. 7. Energy plot in the main counter of π^+ mesons, (a) with absorber out, (b) with absorber in, for the liquid hydrogen run. These π^+ mesons decayed between time of $\sim 2.0 \times 10^{-8}$ sec and of 5.0×10^{-8} sec. The cutoff at 24 Mev is shown, pions of higher energy pass through the main counter. The μ^+ pulse height is also indicated. [The number of equivalent quanta which produced the pions of (a) and (b) are roughly in the ratio 1.75:1.]

¹⁴ D. H. Stork, Phys. Rev. 93, 868 (1954).

target. It has been shown, due to the falling cross section, that the target correction is relatively small for the pions of energy greater than 6 Mev in the main counter, which are considered here.

The absolute beam calibration was based on the calculated value for the quantameter as given by Wilson.¹⁰ The linearity of the integrator system was checked. Cross checks were also made of the quantameter against a Cornell-type chamber. A 2% allowance was made for the finite time-width of the beam in assessing the end-point energy. The synchrotron target was a 0.060-in. diam tungsten wire. Because the dominant radiation arises from the initial few thousandths of an inch (cf. Powell *et al.*¹⁵), the bremsstrahlung spectrum would differ from that of a thin target by at most 3%. The thin-target bremsstrahlung spectrum has been used here.

4. ANALYSIS AND DISCUSSION

Three energy bands were selected from the meson energy plot [Fig. 7(a)], obtained with no absorber, spanning in all, an energy band of roughly 6–23.5 Mev. One energy band only was selected from the plot obtained with absorber [Fig. 7(b)]; to minimize possible scattering errors this was chosen to be 10–23.5 Mev, and these mesons would have energies roughly in the range 32–40 Mev before entering the absorber. To obtain the yield from the liquid hydrogen target, the small number of inverses (1%) and background counts (~12%), referred to previously, were appropriately subtracted. Allowance was then made for the pion energy lost in the thin scintillator and target. After computing the fraction of π^+ mesons which decay in the observed time interval on which Fig. 7 was based, viz. 0.313, and applying the various corrections referred to in the previous paragraph, values were obtained for the differential cross sections as listed in Table I. The error limits refer to relative values (i.e., all uncertainties other than in beam calibration) and arise mainly through statistical considerations. Due to uncertainties in the beam calibration an error in the absolute cross section could occur in addition, which could shift the experimental points as a whole; the absolute calibration error for quantameters has been

TABLE I. Differential cross sections.

Lab. γ -ray energy (Mev)	$d\sigma/d\Omega(10^{-30} \text{ cm}^2/\text{sr})$	$\frac{d\sigma}{d\Omega} \frac{\mu^2}{p\epsilon} \left(1 + \frac{\omega}{M}\right)^2$ ($10^{-30} \text{ cm}^2/\text{sr}$)	θ
162	5.42 ± 0.38	20.0 ± 1.4	82°
168	5.77 ± 0.41	16.4 ± 1.2	79°
175	6.74 ± 0.47	15.6 ± 1.1	76°
192	8.22 ± 0.58	13.6 ± 1.0	73°

¹⁵ W. Powell, W. Hartsough, and M. Hill, Phys. Rev. 81, 213 (1951).

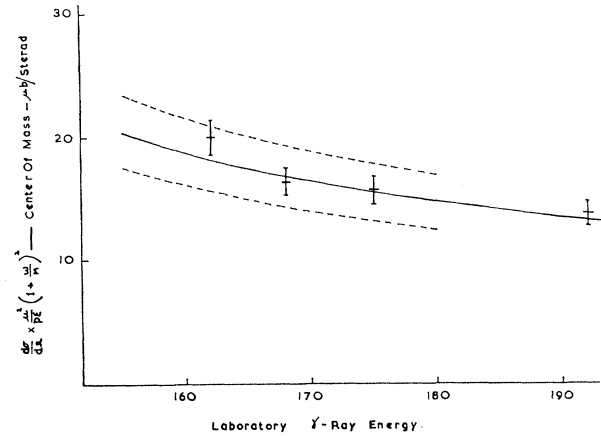


FIG. 8. Experimental plot of $(d\sigma/d\Omega)(1+\omega/M)^2(\mu^2/p\epsilon)$ with energy for 58° laboratory angle, where the error limits refer to relative cross sections. The main curve—is the single dispersion relation (C.G.L.N.) for this laboratory angle as calculated by Robinson. The main curve also corresponds approximately, by chance, to Ball's double-dispersion one for 90° center of mass (cf. text). Also shown are Ball's curves for $\Delta = \pm 1.8e$. Within the errors of absolute calibration the results are compatible with the $\Delta = 0$ curve rising to a threshold value for a_0^+ near $20 \mu\text{b/steradian}$.

discussed by DeWire¹⁶; it was believed on the evidence presented there to be of the order of 5% or less.

These results accord with those of our previous determination (made at 170–185 Mev) within the error limits quoted there. The deduced value of $(d\sigma/d\Omega)(\mu^2/p\epsilon)(1+\omega/M)^2$ which is a measure of the matrix element, is also tabulated, and its value is seen to rise towards threshold. The relevant center-of-mass angles are also shown. These values are shown plotted in Fig. 8. The solid curve, shown for comparison, is the single dispersion relation of Chew, Goldberger, Low, and Nambu⁴ calculated by Robinson¹⁷ for the laboratory angle of 58° used here.

The solid curve also corresponds closely, somewhat fortuitously, to the double dispersion curve of the Mandelstam representation, from the work of Ball⁵ for a center of mass angle of 90° . To compare this latter double-dispersion curve, therefore, with the results of the present experiment, allowance should be made for possible anisotropy near threshold:

$$\frac{d\sigma}{d\Omega} = \frac{p\epsilon}{\mu^2(1+\omega/M)^2} (a_0^+ + a_1^+ \cos\theta + a_2^+ \cos^2\theta + \dots). \quad (2)$$

According to the recent results of Adamovich *et al.*,¹⁸ the anisotropy is small and the allowance from the terms a_1^+ , a_2^+ , ... would be omitted in the γ -ray region

¹⁶ J. W. DeWire, Cornell University Report, Ithaca, New York, 1959 (unpublished).

¹⁷ C. S. Robinson, Illinois University Technical Report, 8, ONR 1834 (05) (unpublished).

¹⁸ See Adamovich, Kharlamov, Gorrhevskaia, Larionova, Yagudha, and Popova (A. M. Baldin, *Proceedings of the 1960 Annual International Conference on High-Energy Physics at Rochester* (Interscience Publishers, Inc., New York, 1960), p. 26.

considered here. Also shown in the diagram are the double-dispersion curves based on a small $\pi-\pi$ coupling term of strength $\Lambda = +1.8e$ or $\Lambda = -1.8e$ for 90° center-of-mass angle (cf. Ball⁵).

It is seen therefore that the results establish a rising trend towards threshold in general accord with the predictions of the theory. Within the errors of the absolute calibration the results are seen to be compatible with the curve based on an f^2 value of 0.08 and $\Lambda=0$, rising to a threshold value for a_0^+ near $20 \mu\text{b/sr}$. It would also seem that the strength of the $\pi-\pi$ coupling does not lie outside the limits shown in Fig. 8, for the value of the coupling constant assumed.

Such a threshold value for a_0^+ in conjunction with π^-/π^+ photoproduction and Panofsky ratio data would

give meson scattering values consistent with the observed S -wave shifts (cf. Hamilton and Woolcock¹⁹).

ACKNOWLEDGMENTS

We would like to express our sincere thanks to Dr. W. McFarlane, and the synchrotron technicians, in particular Mr. T. Elder and Mr. J. Mellor, for providing us with an excellent beam, and to Miss E. Muldoon for her valuable assistance throughout the work. We are grateful to Mr. T. Aitken for help on beam monitors and to Professor P. I. Dee for his interest. One of us (D.W.G.S.L.) thank Department of Scientific and Industrial Research for a maintenance grant.

¹⁹ J. Hamilton and W. S. Woolcock, Phys. Rev. **118**, 291 (1960).

FIG. 4. Some of the filmed $\pi^+ \rightarrow \mu^+$ traces observed with no absorber. (The pulses have a full width of about 10^{-8} sec at half height.)

